Christopher A. Whitfield
Mechanical and Nuclear Engineering Department,
The Pennsylvania State University,
University Park, PA 16802
e-mail: christopher.whitfield@pw.utc.com

Robert P. Schroeder
Mechanical and Nuclear Engineering Department,
The Pennsylvania State University,
University Park, PA 16802
e-mail: rschroeder@psu.edu

Karen A. Thole
Mechanical and Nuclear Engineering Department,
The Pennsylvania State University,
University Park, PA 16802
e-mail: kthole@engr.psu.edu

Scott D. Lewis
Pratt & Whitney,
400 Main Street,
East Hartford, CT 06118
e-mail: scott.lewis@pw.utc.com

Blockage Effects From Simulated Thermal Barrier Coatings for Cylindrical and Shaped Cooling Holes

Film cooling and sprayed thermal barrier coatings (TBCs) protect gas turbine components from the hot combustion gas temperatures. As gas turbine designers pursue higher turbine inlet temperatures, film cooling and TBCs are critical in protecting the durability of turbomachinery hardware. One obstacle to the synergy of these technologies is that TBC coatings can block cooling holes when applied to the components, causing a decrease in the film cooling flow area thereby reducing coolant flow for a given pressure ratio (PR). In this study, the effect of TBC blockages was simulated on film cooling holes for widely spaced cylindrical and shaped holes. At low blowing ratios for shaped holes, the blockages were found to have very little effect on adiabatic effectiveness. At high blowing ratios, the area-averaged effectiveness of shaped and cylindrical holes decreased as much as 75% from blockage. The decrease in area-averaged effectiveness was found to scale best with the effective momentum flux ratio of the jet exiting the film cooling hole for the shaped holes. [DOI: 10.1115/1.4029879]

Introduction

Film cooling is a widely used technology with the purpose of cooling airfoils and improving component durability in a gas turbine. Cool air from the compressor bypasses the combustor and exits through discrete film cooling holes creating a protective layer of fluid between airfoil surfaces and the hot combustion gases. TBCs are another technology used to insulate the airfoils from the hot combustion gases. Very few studies have looked at the impact that these two technologies have on one another. One study by Bunker [1] found that TBCs can significantly alter the initial design geometry of the cooling holes and lower the adiabatic effectiveness relative to an unsprayed hole.

Most laboratory film cooling studies involve holes that are pristine, unaltered from their initial design. In engine hardware, holes are typically machined using a laser, electric discharge machining, or waterjet process, and coatings subsequently alter the hole geometry. TBCs are applied with either an air-plasma spray (APS) or electron beam-physical vapor deposition process. In the current study, a method was developed to spray a low conductivity material into film cooling holes in a line-of-sight manner to simulate an APS process.

Adiabatic effectiveness measurements were performed on both cylindrical and shaped holes placed in a flat plate for a range of conditions. Measurements were made for both cylindrical and shaped holes before and after the holes were sprayed at matched blowing ratios (M) and matched PRs, which simulates more closely what would happen in an engine. Tests were performed at two density ratios (DR = 1.2 and 1.5). This paper also provides a method for scaling the blockage effects for the shaped cooling hole results.

Relevant Past Studies

There have been many studies examining film cooling, but in most studies the holes under consideration were pristine as manufactured. Pristine holes do not normally occur in an actual engine for a variety of reasons including deposition, manufacturing effects, and TBC sprays. Bogard et al. [2] showed the cross section of a film cooling hole with a blockage due to foreign material deposition (Fig. 1).

Experimental studies have shown the detrimental effects on adiabatic effectiveness of in-hole blockages in cylindrical film cooling holes. Jovanovic et al. [3] found significant changes in the flowfield of a cylindrical hole blocked with a half torus shaped blockage, which is commonly found in the melt ejection during laser drilling. Large decreases in film cooling effectiveness were also found, with the decreases being larger at low velocity ratios. The half torus shape differs from that of sprayed blockages considered in the current study, since sprayed blockages sit only on the floor of the hole outlet. A study by Demling and Bogard [4] saw decreases in adiabatic effectiveness of up to 80% compared to unblocked holes for blockages that were half the hole diameter, placed inside holes on the suction side of a vane. Sundaram and Thole [5] found that an in-hole blockage of $t/D = 0.3$ reduced area-averaged effectiveness by nearly 30% over a row of five holes on a vane endwall.

Computational studies have also indicated that hole blockages reduce adiabatic effectiveness. The study by Na et al. [6] ran simulations on unblocked and blocked cylindrical holes. Blocked holes were found to decrease film effectiveness, though this reduction was minimized by lowering the mass flow rate through the hole. Na et al. attributed this behavior to the geometry of the simulated TBC blockage.

To the best of our knowledge, only one experimental study has examined the detrimental effects of a TBC coatdown on film

Fig. 1 Micrograph of a blocked film cooling hole from Bogard et al. [2]

Contributed by the International Gas Turbine Institute (IGTI) of ASME for publication in the JOURNAL OF TURBOMACHINERY. Manuscript received July 14, 2014; final manuscript received December 1, 2014; published online March 10, 2015. Editor: Ronald Bunker.

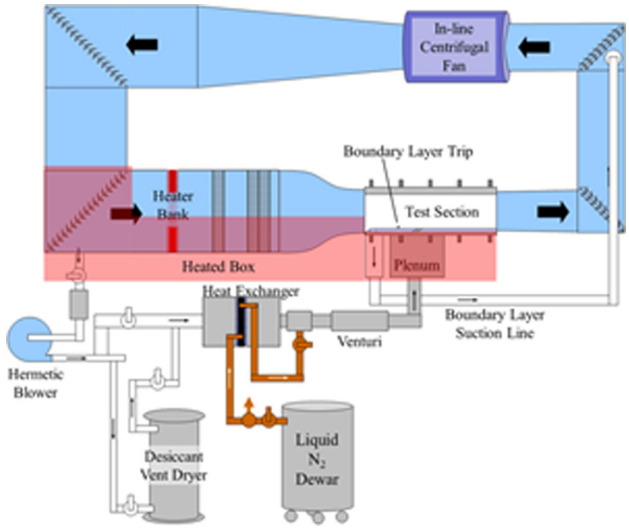

Fig. 2 Schematic of wind tunnel used in the current study

cooling performance. Bunker [1] measured adiabatic film effectiveness for cylindrical and shaped holes with an APS applied TBC coating of $t/D = 0.4$. He presented results only in terms of the centerline adiabatic effectiveness levels. Bunker found that this blockage resulted in a 50% reduction in centerline effectiveness at $M = 1$ for all $x/D < 50$ in cylindrical holes and a 30% reduction for all $x/D < 20$ in shaped holes at $M = 1$ and 1.2. Shaped hole centerline effectiveness recovered to unblocked values past $x/D = 40$.

Experimental Facility and Test Matrix

All adiabatic effectiveness measurements were taken in a closed-loop wind tunnel shown in Fig. 2, which was previously described by Eberly and Thole [7]. Mainstream air was circulated at 10 m/s by an in-line centrifugal fan. The mainstream air was thermally conditioned by a bank of electrical heating elements as well as by a chilled water heat exchanger. At the entrance to the test section, a suction loop removed the incoming boundary layer. A new boundary layer originated at the leading edge of the test plate before being tripped to initiate transition to a turbulent state. A wire 1.2 mm in diameter located approximately 33D upstream of the film cooling holes was used for this purpose. Characteristics of the boundary layer 1.3D upstream of the film cooling holes are given in Table 1 [7].

Coolant air for the film cooling injection was diverted from the mainstream flow by a 60 Hz variable frequency blower that was hermetically sealed. The coolant air was sent through solid desiccant to dry the air before cooling to cryogenic temperatures. The closed loop design of the tunnel ensured that the mainstream was also dry. Adiabatic effectiveness and pressure measurements were not recorded if condensate was observed on the test plate. Downstream of the desiccant, the coolant air passed through a heat exchanger cooled by liquid nitrogen. After the heat exchanger, the evaporated nitrogen was mixed directly into the coolant flow to provide additional cooling. The coolant flow rate was then measured by a Venturi flow meter before entering a plenum. The interior of the plenum contained three conditioning screens to ensure uniformity before the flow reached the inlet to the film cooling

Table 1 Boundary layer characteristics

θ/D	δ/D	Re_θ	Re*
0.13	1.2	670	315

Table 2 Description of cylindrical and shaped holes

Hole type	α	β_{fwd}	β_{lat}	L/D	P/D	w/P	AR	D
Cylindrical	30 deg	—	—	4.7	6.67	0.15	1	8.2 mm
Shaped	30 deg	7 deg	7 deg	6	6	0.35	2.5	7.7 mm

holes. Density ratios of DR = 1.2 and 1.5 were matched in this study.

Film cooling holes were machined out of Dow Styrofoam brand residential sheathing to provide a nearly adiabatic surface ($k = 0.029$ W/m·K). Table 2 and Fig. 3 fully describe the geometries of the cylindrical and shaped holes blocked in the current study. The shaped 7-7-7 hole geometry (which will be referred to as the shaped hole in this paper) is a laidback-fanshaped hole representative of shaped holes in open literature. It features a cylindrical metering section ($L_{\mathrm{inlet}}/D = 2.5$) which then expands into a diffused outlet via 7 deg expansion angles in the forward and lateral (half-angle) directions. This shaped hole design may be downloaded at the website of the authors' research group [8]. Baseline adiabatic effectiveness performance for the shaped hole was given by Schroeder and Thole [9].

While there are multiple industrial processes which apply TBC to an airfoil, the current study simulates an APS process much like that presented by Bunker [1]. This process was chosen due to the line-of-sight manner in which material is deposited on the surface. The simulated TBC coating in the test coupons was sprayed by atomizing a foam sealant ($k = 0.036$ W/m·K). The spray was applied perpendicular to the surface of the plate to ensure that the spray deposited in film cooling holes in a realistic and repeatable pattern. To keep the remainder of the surface of the plate clean, a mask was used. When completed, the top surface of blockages was flush with the test surface. A backward step feature would exist on the upstream edge of the hole breakout in actual engine application. Adiabatic effectiveness measurements were taken, separate from this study, for holes with and without this upstream edge feature. Results indicated that for blowing ratios of 2.0 and below, the upstream step feature had a minimal impact on adiabatic effectiveness.

Cross sections of cylindrical and shaped holes were cut and the photographs are shown in Figs. 3(*a*) and 3(*b*), respectively. The

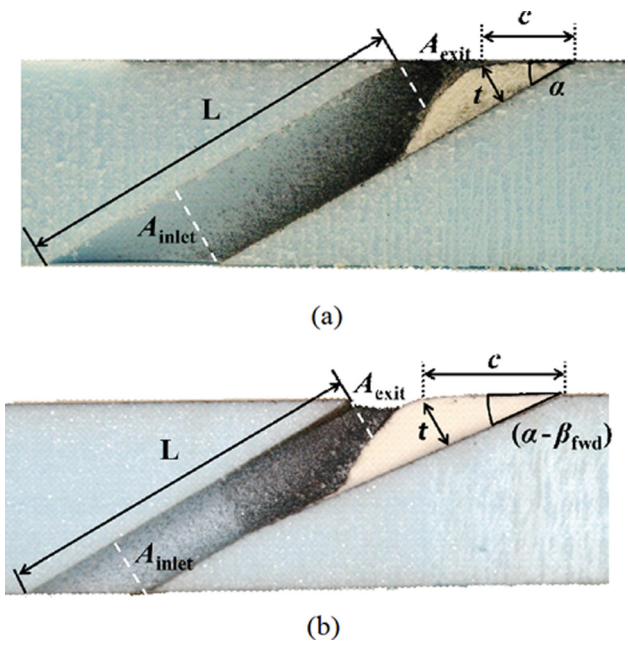

Fig. 3 Cross sections of (*a*) a blocked cylindrical hole and (*b*) a blocked shaped hole

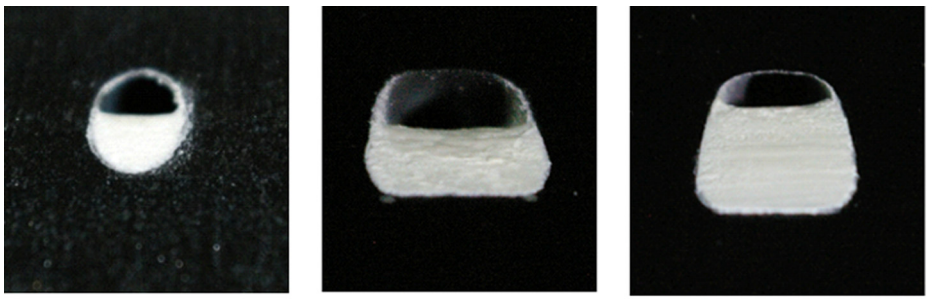

Fig. 4 Axial photographs of the blocked hole exits of (*a*) a cylindrical hole with a *t/D* = 0.5 blockage, (*b*) a shaped hole with a *t/D* = 0.5 blockage, and (*c*) a shaped hole with a *t/D* = 0.9 blockage

Table 3 Configurations of simulated TBC coatings tested

Hole type	*t/D*	AR_{eff}	Change in exit area from unblocked	Location of minimum flow area
Shaped	Unblocked	2.5	—	Inlet
Shaped	0.5	1.8	−29%	Inlet
Shaped	0.9	1.2	−52%	Inlet
Cylindrical	Unblocked	1	—	Anywhere in hole
Cylindrical	0.5	0.65	−35%	Exit

thicknesses of the deposits were characterized using geometric relationships given in Figs. 3(*a*) and 3(*b*). The thickness of the cylindrical hole blockage is given by the following equation:

$$t = c * \sin(\alpha) \tag{1}$$

The blockage thicknesses were found for the shaped hole using the same equation with the appropriate inclination angle. Photographs of the outlets of blocked cylindrical and shaped holes are shown in Fig. 4.

Table 3 displays blockage configurations used in the current study. The cylindrical hole blockage of $t/D = 0.5$ was chosen to approximately match in-hole blockages of Demling and Bogard [4] as well as Bunker [1]. Two blockage thicknesses were tested in shaped holes, $t = 0.5D$ and $t = 0.9D$. The larger blockage reduced the exit area of the shaped holes by 52%, up from 29% for the $t/D = 0.5$ blockage. These reductions in the area of the exit plane were calculated based on the cross sections shown in Fig. 3. The blockages in the shaped holes were only present in the expanded portion of the shaped hole. No simulated TBC deposited in the metering section of the shaped holes.

Table 3 also gives the effective area ratio (AR_{eff}). The AR_{eff} is meaningful because it is needed to determine an effective momentum flux ratio (I_{eff}), as shown below:

$$I_{eff} = \frac{\rho_c U_{exit}^2}{\rho_\infty U_\infty^2} = \frac{\rho_c}{\rho_\infty U_\infty^2} * \left(\frac{U_c}{AR_{eff}}\right)^2 = \frac{I}{AR_{eff}^2} \tag{2}$$

For configurations where the exit area equaled the inlet area, $AR_{eff} = 1$ and I_{eff} equals the momentum flux ratio in the metering section. Blocked holes had a higher effective momentum flux ratio than unblocked holes at the same coolant flowrate. The effect of momentum flux ratio on jet detachment and heat transfer has been studied by Thole et al. [10] and Sinha et al. [11].

Adiabatic effectiveness measurements were determined from surface temperature measurements made with a FLIR SC620 infrared camera. The camera output was calibrated to detect accurately the entire range of temperatures measured, similar to the method employed by Eberly and Thole [7]. Coolant and freestream temperatures were each measured using multiple thermocouples.

Pressure measurements were also made to evaluate the discharge coefficients for the unblocked and blocked cooling holes. Pressures were measured in the coolant plenum as well as in the mainstream using static pressure taps.

Table 4 shows all of the test conditions and blockage configurations for cylindrical and shaped holes. Blocked holes were evaluated at both blowing-ratio-matched and pressure-ratio-matched conditions for each nominal test condition.

Uncertainty Analysis

An uncertainty analysis was performed for unblocked and blocked holes at both DR = 1.2 and DR = 1.5. All uncertainty values reported are for a 95% confidence level and are based on propagating uncertainties using the method of partial derivatives as found in Figliola and Beasley [12]. The uncertainty in DR was at most ± 1.2% for DR = 1.5 and ±0.8% for DR = 1.2. The maximum value of uncertainty in η was dominated by the bias error in plenum thermocouples and was found to be ±0.024 for DR = 1.5 tests and ±0.032 for DR = 1.2 tests. At the very lowest blowing ratio tested ($M = 0.26$), the uncertainty in M was ±22%, but decreased to ±10% at $M = 0.5$. This high uncertainty was due to such a low flowrate though the Venturi flow meter. At the highest blowing ratio of $M = 3.0$, the uncertainty was ±1.6%.

Table 4 Blowing ratios tested

		Blocked ($t/D = 0.5$)		Blocked ($t/D = 0.9$)	
Hole type	Unblocked	*M* match	PR match	*M* match	PR match
Cylindrical DR = 1.2	0.51	0.50	0.29	—	—
	0.72	0.74	0.44	—	—
	1.03	1.00	0.56	—	—
Cylindrical DR = 1.5	0.53	0.53	0.26	—	—
	0.78	0.75	0.51	—	—
	1.03	1.02	0.63	—	—
Shaped DR = 1.2	0.51	0.50	0.45	—	—
	0.99	0.98	0.92	—	—
	2.00	1.99	1.91	—	—
Shaped DR = 1.5	0.52	0.49	0.44	0.50	0.35
	—	—	—	0.62	—
	1.00	1.00	0.93	0.99	0.79
	1.51	—	—	—	1.24
	2.01	1.99	1.97	2.00	1.68
	2.50	—	—	—	—
	3.02	—	—	3.01	—

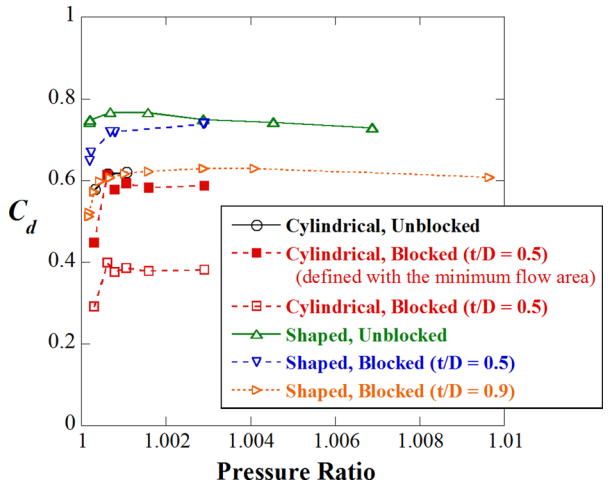

Fig. 5 Discharge coefficients for cylindrical and shaped holes at DR = 1.5

The uncertainty in the effective AR was determined for blocked holes by cutting cross sections of the holes and measuring the percentage of outlet flow area blocked by the spray. The uncertainty in AR_{eff} was ±4% at most for any blocked hole. For cylindrical holes, this led to uncertainty in I_{eff} of ±19% for the DR = 1.5 and $M = 0.5$ blocked hole test, and ±12% for the DR = 1.5 and $M = 1.0$ blocked hole test.

The uncertainty in discharge coefficient was found to be at most ±22% and occurred at the lowest flowrates. Discharge coefficient uncertainty was heavily dependent on the uncertainty of mass flow rate though the hole. At the highest flowrates, the uncertainty in C_d was ±1.6%.

Measured Discharge Coefficients

Incompressible discharge coefficients (C_d) were calculated from pressures measured in the plenum and freestream for each test performed. Comparisons were made to the literature for the baseline case of a cylindrical hole with no blockage. For a pressure ratio of PR = 1.0006, $C_d = 0.62$, which agreed with that given by Burd and Simon [13] within 2%.

Figure 5 shows the C_d for all DR = 1.5 tests performed in the current study for both cylindrical and shaped holes as a function of the PR. All holes had a minimum flow area equal to the inlet area, except the blocked cylindrical holes. Figure 5 shows the C_d for the blocked cylindrical holes based on two different areas: the inlet area and the minimum flow area. This was done because the inlet area was always known, whereas the exit area was not known for a blocked hole until destructive methods were used to find the exit area.

Shaped holes with the $t/D = 0.5$ blockage experienced only a small decrease in discharge coefficient, remaining well above the discharge coefficient values for unblocked cylindrical holes. There was a much larger decrease in C_d for the $t/D = 0.9$ blockage. Figure 5 illustrates that the $t/D = 0.9$ blockage decreased the C_d in shaped holes to that of unblocked cylindrical holes, despite their 20% difference in area ratio ($AR_{eff} = 1.2$ and $AR = AR_{eff} = 1.0$, respectively).

One might expect the decrease in C_d to match the decrease in exit area, but this was not the case. The large blockage of $t/D = 0.9$ lowered the average discharge coefficient from $C_d = 0.75$ to 0.60, a reduction of about 20%. This drop was significantly less than the 52% reduction in exit area that was caused by the blockage.

Blockage Effects on Cylindrical Hole Cooling

Adiabatic effectiveness contours for unblocked and blocked cylindrical holes can be seen for DR = 1.5 and $M = 0.5$ (Figs. 6(*a*)–6(*c*)) and $M = 1$ (Figs. 7(*a*)–7(*c*)). It is important to note that the matched PR cases have much lower blowing ratios than the unblocked cases, which follows from the decreases in discharge coefficients previously discussed. The matched PR cases, however, are representative of what would occur in an engine since the PR across the holes is constant.

By comparing the unblocked and blocked tests in Figs. 6(*a*)–6(*c*), one can clearly see that the blocked holes did not distribute the coolant across the surface as well as the unblocked case at $M = 0.5$. The PR matched case in which $M = 0.26$ (Fig. 6(*b*)) showed much better coolant distribution than the case of matched blowing ratio (Fig. 6(*c*)), even though the coolant flowrate is only

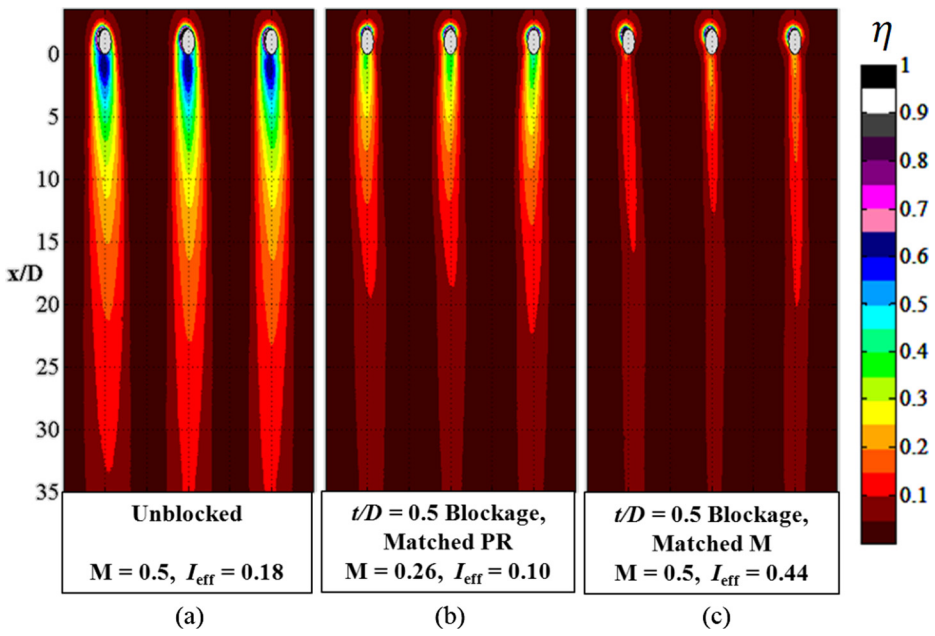

Fig. 6 Cylindrical hole adiabatic effectiveness contours for DR = 1.5 and $M = 0.5$: (*a*) unblocked hole—$M = 0.5$ and $I_{eff} = 0.18$, (*b*) blocked hole with matched PR—$M = 0.26$, $I_{eff} = 0.10$, and $t/D = 0.5$, and (*c*) blocked hole with matched M—$M = 0.5$, $I_{eff} = 0.44$, and $t/D = 0.5$

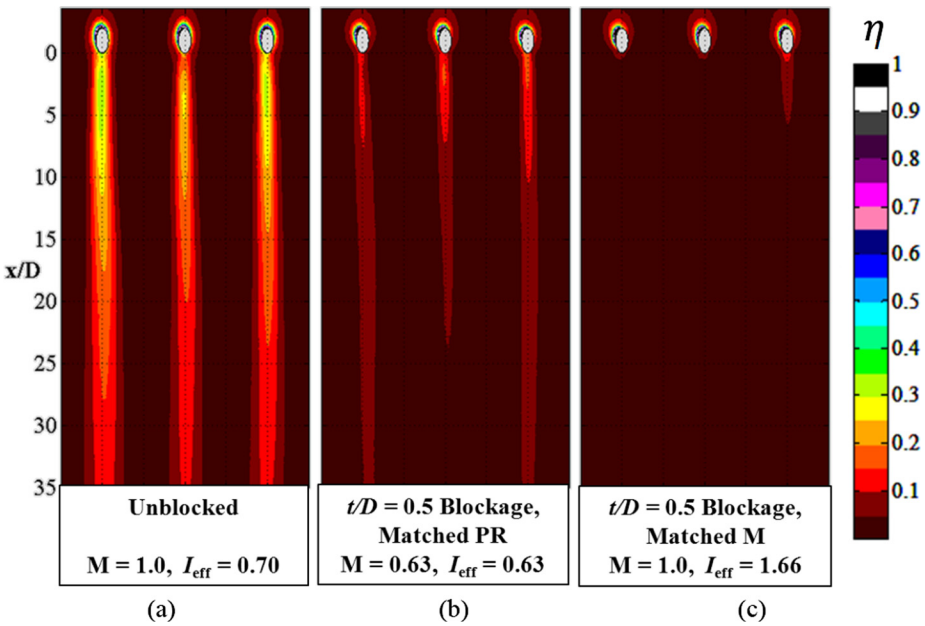

Fig. 7 Cylindrical hole adiabatic effectiveness contours for DR = 1.5 and $M = 1$: (*a*) unblocked hole—$M = 1.0$ and $I_{eff} = 0.70$, (*b*) blocked hole with matched PR—$M = 0.63$, $I_{eff} = 0.63$, and $t/D = 0.5$, and (*c*) blocked hole with matched M—$M = 1.0$, $I_{eff} = 1.66$, and $t/D = 0.5$

half ($M = 0.26$ versus $M = 0.5$). For the matched blowing ratio case (Fig. 6(*c*)), there was a much higher effective momentum flux ratio of $I_{eff} = 0.44$, causing the onset of jet detachment.

Cylindrical hole results at the highest blowing ratio of $M = 1$ are shown in effectiveness contours in Figs. 7(*a*)–7(*c*). For this high blowing ratio case, jet detachment and reattachment was apparent for the unblocked and PR matched cases. These cases, presented in Figs. 7(*a*) and 7(*b*), both have similar I_{eff} values which fall in the $0.4 < I < 0.8$ range stated by Thole et al. [10] to show detachment and reattachment. For the PR matched case, the coolant footprint on the surface was narrower than the unblocked case, owing to the lower cooling capacity with the reduced blowing ratio $M = 0.63$. Coolant was completely detached for the matched blowing ratio case (Fig. 7(*c*)), which had very high jet momentum ($I_{eff} = 1.66$). This momentum flux ratio was more than twice the value associated with the point at which most jets detach from the surface.

Figures 8(*a*)–8(*c*) show laterally averaged effectiveness for three blowing ratios at DR = 1.5. Note that even though the absolute effectiveness levels for the three cases decreased with increasing blowing ratio, the relative distribution of the levels is strikingly similar. PR matched cases had higher laterally averaged effectiveness values than blowing ratio matched cases. The PR matched tests suffered a 30–50% decrease in performance relative to unblocked, while the blowing ratio matched tests showed a decrease of 50% or more at all x/D values.

Blockage Effects on Shaped Hole Cooling

Figures 9(*a*)–9(*c*) show adiabatic effectiveness contours for the shaped holes at the lowest blowing ratio, $M = 0.5$, for both small and large blockages all at a matched blowing ratio. Figures 10(*a*)–10(*c*) show adiabatic effectiveness contours for the shaped holes at the lowest blowing ratio for the case of a matched PR. The blowing ratio did not decrease as significantly for the matched PR case as it did for the cylindrical holes at the same $t/D = 0.5$ blockage.

As the blockage increased from $t/D = 0.5$ to $t/D = 0.9$, Figs. 9(*a*)–9(*c*) show that the coolant contours became slightly narrower but the centerline values extended farther downstream. Careful

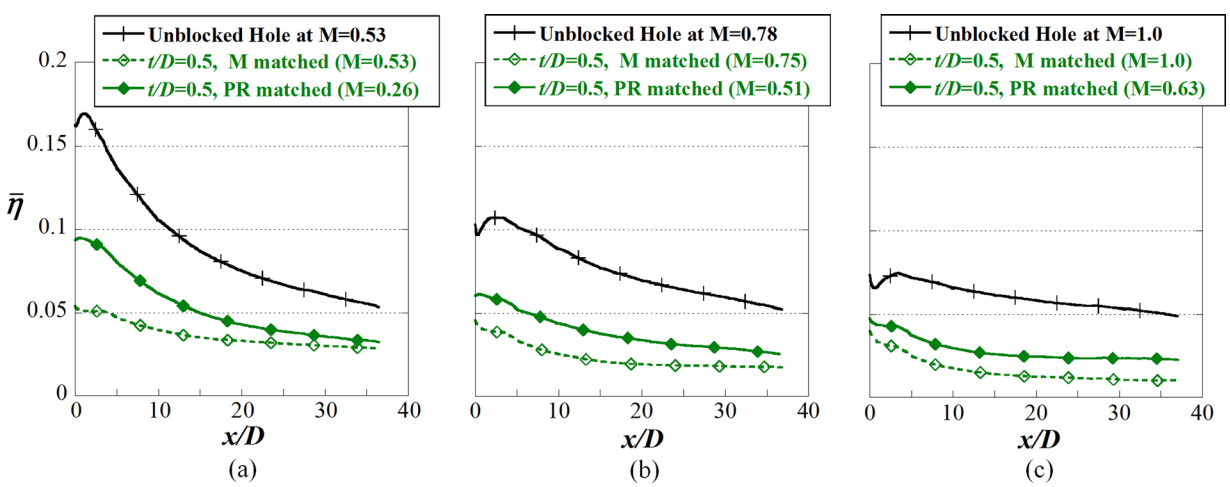

Fig. 8 Cylindrical hole DR = 1.5 laterally averaged effectiveness at (*a*) $M = 0.5$, (*b*) $M = 0.75$, and (*c*) $M = 1.0$

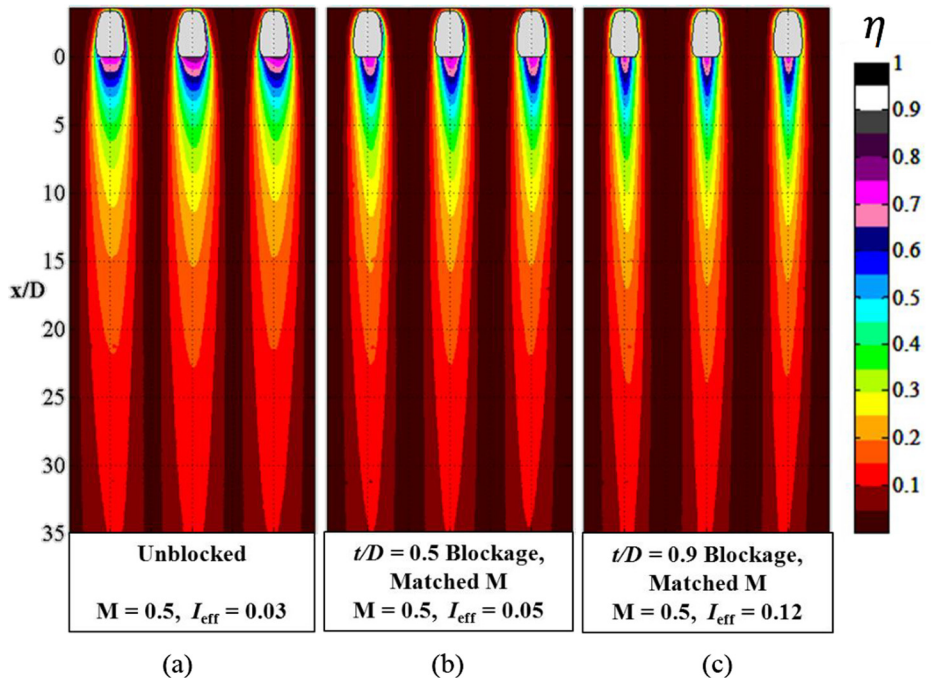

Fig. 9 Shaped hole adiabatic effectiveness contours for DR = 1.5 and $M = 0.5$ matched M cases: (*a*) unblocked hole—$M = 0.5$ and $I_{eff} = 0.03$, (*b*) $t/D = 0.5$ blockage—$M = 0.5$ and $I_{eff} = 0.05$, and (*c*) $t/D = 0.9$ blockage—$M = 0.5$ and $I_{eff} = 0.12$

inspection of the adiabatic effectiveness contours reveals that a given contour level extends further downstream for the blocked holes than for the unblocked holes. The narrowing can be explained by a reduction in the breakout width of the hole with the blockage present. In this study, effective breakout width (w) was defined as the widest lateral width of the hole breakout (the blocked part of the hole was not considered part of the effective breakout). The coverage ratio (w/P) for the shaped holes in this study ranged from $w/P = 0.35$ for unblocked holes to $w/P = 0.27$ for the larger, $t/D = 0.9$ blockage.

Figures 10(*a*)–10(*c*) show effectiveness contours where PR was matched for the low blowing ratio case. Matching PR led to a blowing ratio of $M = 0.44$ for the $t/D = 0.5$ blockage and $M = 0.35$ for the $t/D = 0.9$ blockage. Similar to the matched M cases in Figs. 9(*a*)–9(*c*), increased blockage caused reduced coolant spreading. But unlike the matched blowing ratio cases, Figs.

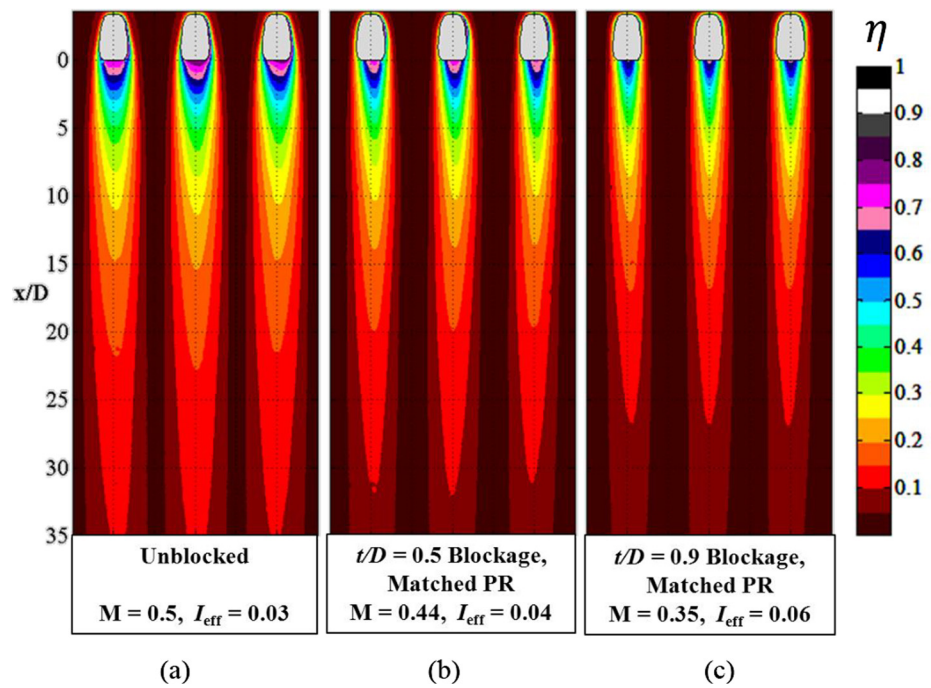

Fig. 10 Shaped hole adiabatic effectiveness contours for DR = 1.5 and $M = 0.5$ matched PR cases: (*a*) unblocked hole—$M = 0.5$ and $I_{eff} = 0.03$, (*b*) $t/D = 0.5$ blockage—$M = 0.44$ and $I_{eff} = 0.04$, and (*c*) $t/D = 0.9$ blockage—$M = 0.35$ and $I_{eff} = 0.06$

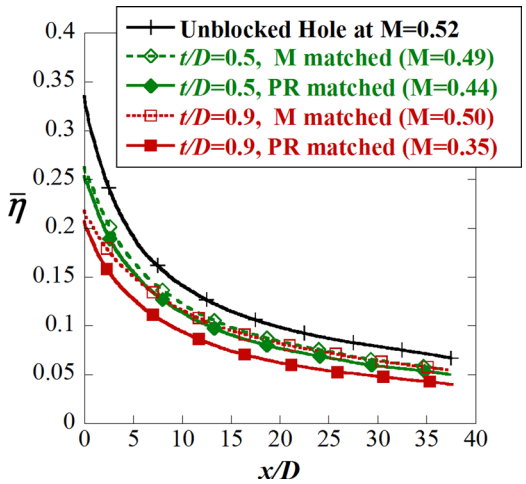

Fig. 11 Shaped hole laterally averaged effectiveness for DR = 1.5 and $M = 0.5$

10(*a*)–10(*c*) show that the centerline effectiveness decreased with increasing blockage. This decrease in the centerline values can be explained by the fact that there was a reduction in coolant mass-flow for the matched PR cases.

Figure 11 shows laterally averaged effectiveness for all five cases at $M = 0.5$ (unblocked, two different blockages with matched blowing ratio, and two blockages with matched PR). Note that the vertical scale in these plots extends to $\bar{\eta} = 0.4$ instead of 0.2, due to better performance than the cylindrical holes shown earlier. Larger blockages caused slightly decreased laterally averaged effectiveness. The PR matched cases performed worse than blowing ratio matched cases due to the reduced blowing ratio and therefore cooling capacity. This difference was more apparent with the $t/D = 0.9$ blockage where the PR match led to a 30% decrease in mass flow through the hole.

Adiabatic effectiveness for the shaped hole was generally higher at $M = 1$ compared to the $M = 0.5$ cases, especially far downstream of the holes as shown by the contours in Figs. 12(*a*)–12(*d*). As was discussed, for the small blockage there was little change in the discharge coefficient such that the matched *M* and *PR* were identical. At $M = 1$, large differences in cooling performance are seen with the two blockage sizes. It is evident that the blowing ratio matched case with the $t/D = 0.9$ blockage led to much lower effectiveness than with the $t/D = 0.5$. For DR = 1.5 and $M = 1$, the $t/D = 0.5$ blockage caused reduction in lateral spreading of coolant but not a reduction in centerline effectiveness. In contrast, the $t/D = 0.9$ blockage caused a decrease in centerline effectiveness as well as in lateral spreading. Also noteworthy is that the matched PR case for the $t/D = 0.9$ blockage (Fig. 12(*c*)) had greater effectiveness and lateral spreading near the hole than the matched blowing ratio case. This was at a 20% reduced mass flux compared to the test in which blowing ratio was matched ($M = 0.8$ versus $M = 1.0$) and represents a reversal of the behavior seen at $M = 0.5$. The reversal indicates that at $M = 1$ the benefit from increased coolant mass flux by matching M instead of PR was counteracted by the increase in the momentum of the coolant jet, momentum that tended to carry the jets away from the surface. The jet momentum at the exit of the hole was represented by the effective momentum flux ratio (I_{eff}). At the $M = 1$ test conditions, the $t/D = 0.9$ blockage resulted in $I_{\text{eff}} = 0.29$ for the PR matched case and $I_{\text{eff}} = 0.46$ for the blowing ratio matched case. In contrast, the effective momentum flux ratio was small in the $M = 0.5$ cases: the greatest was $I_{\text{eff}} = 0.12$ for matched blowing ratio with the $t/D = 0.9$ blockage, which was not enough to cause detrimental coolant penetration into the mainstream.

Adiabatic effectiveness patterns in Figs. 12(*a*)–12(*d*) are comparable to centerline effectiveness data presented by Bunker [1]. Bunker presented unblocked and blocked data at conditions of $M = 1$ for a shaped-hole blockage with $t/D = 0.4$. Bunker found that, due to blockage, centerline effectiveness decreased around 30% near the hole. Figures 12(*a*)–12(*d*) show that in the current study, the $t/D = 0.5$ blockage resulted in only a slight decrease in centerline effectiveness at the $M = 1$ condition, and for the larger $t/D = 0.9$ blockage centerline effectiveness decreased by 30% at worst (at $x/D = 6$) when PR was matched.

Figure 13 shows laterally averaged effectiveness for these DR = 1.5 and $M = 1$ tests. Differences here are greater than those measured at $M = 0.5$. The $t/D = 0.5$ blockage performance was identical between matched blowing or PR and was significantly lower than unblocked performance due to reduced lateral spreading.

Figures 14(*a*)–14(*d*) show effectiveness contours at $M = 2$ for the shaped hole. The reduction in effectiveness was severe with

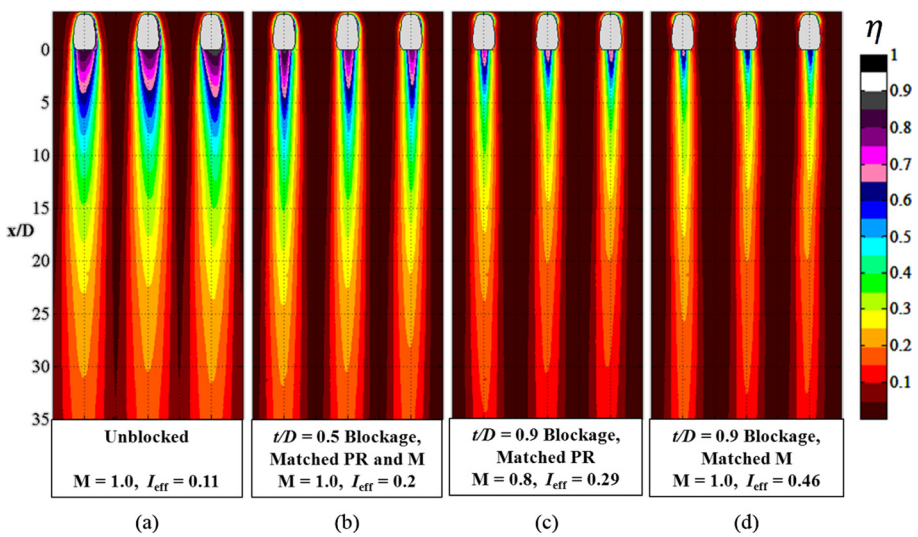

Fig. 12 Shaped hole adiabatic effectiveness contours for DR = 1.5 and $M = 1$: (*a*) unblocked hole—$M = 1.0$ and $I_{\text{eff}} = 0.11$, (*b*) $t/D = 0.5$ blockage, matched PR and *M*—$M = 1.0$ and $I_{\text{eff}} = 0.2$, (*c*) $t/D = 0.9$, matched *PR*—$M = 0.8$ and $I_{\text{eff}} = 0.29$, and (*d*) $t/D = 0.9$, matched *M*—$M = 1.0$ and $I_{\text{eff}} = 0.46$

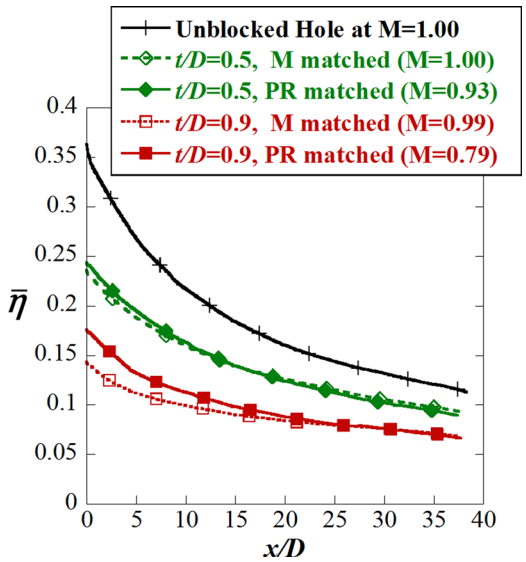

Fig. 13 Shaped hole laterally averaged effectiveness for DR = 1.5 and $M = 1$

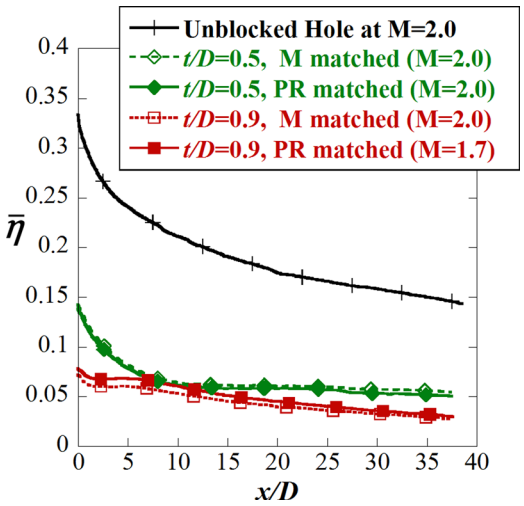

Fig. 15 Shaped hole laterally averaged effectiveness for DR = 1.5 and $M = 2$

both blockages; however, the coolant patterns downstream of the holes were different between the small and large blockages. With the $t/D = 0.5$ blockage, the coolant pattern was narrower than the breakout width of the hole everywhere. The $t/D = 0.9$ blockage also showed a narrow coolant pattern near the hole, but then expanded to a wider coolant footprint downstream. Figure 15 shows the lateral averages indicating that the coolant mixing rate was different for all three cases. With the $t/D = 0.5$ blockage, the adiabatic effectiveness was relatively constant after $x/D = 10$. In contrast, the effectiveness resulting from the $t/D = 0.9$ blockage was low immediately downstream of the holes followed by a gradual decay. The different behaviors with the small and large blockage are understandable considering the large difference in effective momentum flux ratio ($I_{\text{eff}} = 0.84$ with the small blockage, $I_{\text{eff}} \geq 1.3$ with the large blockage). Interestingly, the blocked shaped holes showed no sign of detachment-then-reattachment until flowrates well above $I_{\text{eff}} = 0.8$. This was in contrast to unblocked cylindrical holes which exhibit this behavior in the momentum flux ratio range $0.4 < I = I_{\text{eff}} < 0.8$ [10].

Scaling of Blockage Effects

Area-averaged effectiveness values are presented in Fig. 16(*a*) in which the area used ranged from $3 \leq x/D \leq 19$. Because of the slightly different pitchwise spacing between hole types, all cylindrical hole data were normalized by the pitch difference. Blockages reduced both the peak effectiveness values as well as the blowing ratio where the peak was reached for the shaped hole. Larger blockages caused a more dramatic decrease in peak effectiveness and in the blowing ratio of the peak as compared with the smaller blockages for shaped holes. In every case, the shaped hole outperformed the cylindrical hole whether it was blocked or not.

While the blowing ratio is a useful parameter because it represents the rate of coolant flow through the holes, it does not take into account changes at the outlet of the hole due to blockages. To account for these exit area changes, the area-averaged effectiveness was evaluated as a function of I_{eff} as shown in Fig. 16(*b*). Momentum flux ratio is typically used to describe jet detachment from cylindrical holes, but shaped holes with conservative expansion angles are also sensitive to changes in I_{eff}. The peak performance for shaped holes occurred at approximately $I_{\text{eff}} = 0.2$

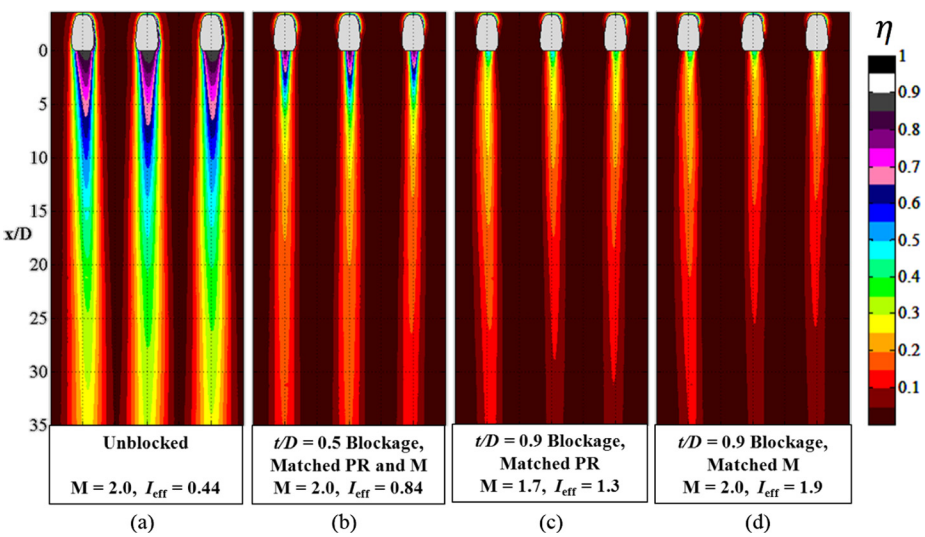

Fig. 14 Shaped hole adiabatic effectiveness contours for DR = 1.5 and $M = 2$: (*a*) unblocked hole—$M = 2.0$ and $I_{\text{eff}} = 0.44$, (*b*) $t/D = 0.5$ blockage, matched PR and M—$M = 2.0$ and $I_{\text{eff}} = 0.84$, (*c*) $t/D = 0.9$ matched PR—$M = 1.7$ and $I_{\text{eff}} = 1.3$, and (*d*) $t/D = 0.9$ matched M—$M = 2.0$ and $I_{\text{eff}} = 1.9$

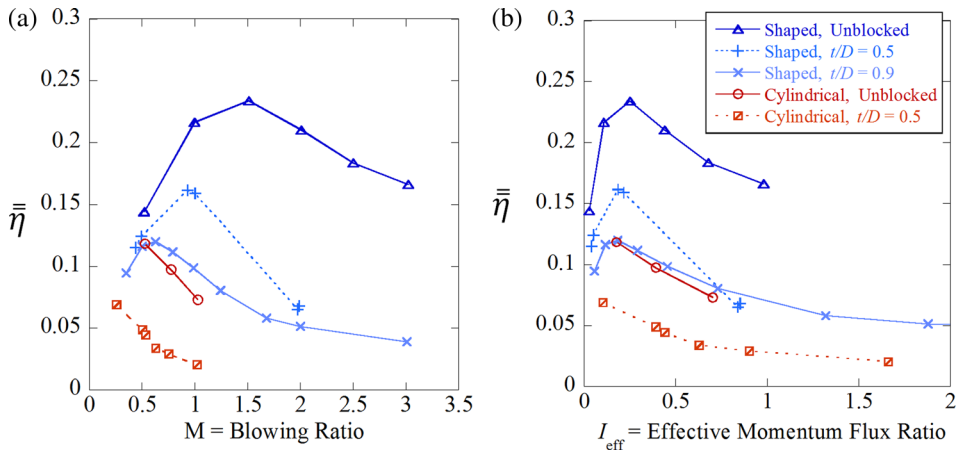

Fig. 16 Area-averaged adiabatic effectiveness at DR = 1.5 versus (*a*) blowing ratio and (*b*) effective momentum flux ratio. For cylindrical holes, $\bar{\bar{\eta}}$ was multiplied by 6.7/6 to account for wider pitchwise spacing.

regardless of blockage thickness. Similar results were seen for cylindrical holes, although at slightly lower I_{eff} values. This is consistent with previous cylindrical hole studies: the highest laterally averaged effectiveness measured by Sinha et al. [11] occurred at momentum flux ratios below $I = I_{\text{eff}} = 0.2$, even though the onset of jet detachment begins at $I = I_{\text{eff}} = 0.4$ as found by Thole et al. [10].

Not only does the peak area-averaged effectiveness scale with the effective momentum flux ratio, but also the I_{eff} correlates the net reductions in area-averaged adiabatic effectiveness from hole blockage. In Fig. 17, the reduction in area-averaged effectiveness for shaped hole blockages at matched PR (solid symbols) and matched blowing ratio (open symbols) is plotted as a function of resulting I_{eff}. The data collapse to a single curve for all of the cases studied for the shaped hole. The $t/D = 0.5$ blockage DR = 1.2 and $M = 2.0$ tests did not agree perfectly with this trend, but all other tests agreed very well. For $I_{\text{eff}} < 1$, the percent change in $\bar{\bar{\eta}}$ became greater with increasing I_{eff} whereas for $I_{\text{eff}} > 1$, the percentage reduction levels off to a constant reduction in effectiveness of around 75%. Overall, the collapse of data is quite remarkable for both matched *PR* and matched *M* cases as well as for different blockage sizes. Although contours were not presented in this paper for brevity's sake, DR = 1.2 tests were performed at the same blowing ratios as DR = 1.5 tests. These data were used to evaluate the scaling of I_{eff} as shown in Fig. 17. Good scaling occurred for both DRs as well.

Similarly, reductions in area-averaged effectiveness were evaluated using I_{eff} for cylindrical hole data as shown in Fig. 18. Note that the trendline curve from the shaped hole data shown in Fig. 17 is repeated in Fig. 18 for comparison. While there is good agreement with the majority of the data, some of the high flowrate data did not collapse onto the curve.

Data points in worst agreement with the curve are circled with a solid circle in Fig. 18. The unblocked momentum flux ratio for these two points was $I = 0.87$, which is in the $I > 0.8$ range corresponding to complete blowoff described by Thole et al. [10]. Points with unblocked I corresponding to the detached-then-reattached range of $0.4 < I < 0.8$ exhibited mixed behavior and are circled with a dashed circle. Some points agreed well with the trendline, and others did not. All points in the attached range ($I < 0.4$), however, fit well with the trendline.

Figure 18 also includes percent reductions in $\bar{\bar{\eta}}$ reported by Demling and Bogard [4,14], for the area 0–18*D* downstream of cylindrical holes. Their measurements were with cylindrical holes on the suction side of a rough-surface vane, with high freestream turbulence of 20% approaching the vane. The tests were carried out at matched PR. Percent reductions ranging from 30% to 80% were observed for an in-hole blockage of size $t/D = 0.5$. The

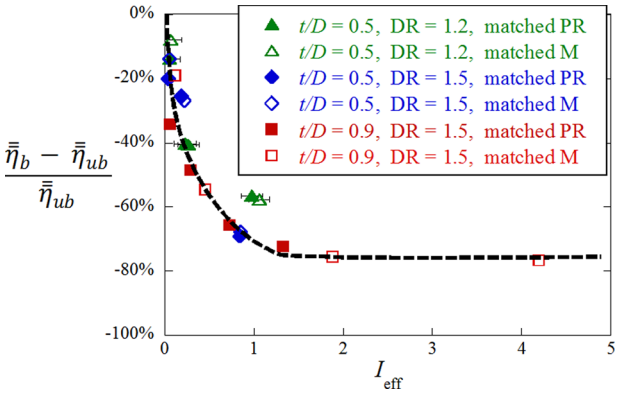

Fig. 17 Percent change in area-averaged effectiveness with shaped hole blockage, as a function of the effective momentum flux ratio

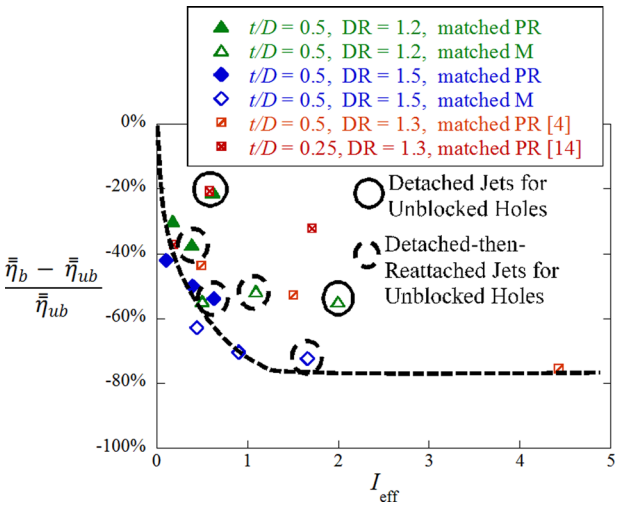

Fig. 18 Percent change in area-averaged effectiveness with cylindrical hole blockage in the current study and in Demling and Bogard [4,14]

authors of the current study estimated I_{eff} for Demling and Bogard data from the given blockage sizes ($t/D = 0.25$ or 0.5). As seen in Fig. 18, percent reductions for Demling and Bogard data were less than those expected from the shaped hole trendline. Their lower

reductions in effectiveness were partially attributed to the high turbulence level in that study, which can improve cooling effectiveness levels in the case of detached jets. This improvement happens as a result of the turbulence transporting cooler fluid closer to the wall.

Conclusions

The effects of blockages on film effectiveness were investigated for both cylindrical and shaped film cooling holes. The particular blockages of interest in this study were those applicable to TBCs resulting from the air-plasma spraying process. The results indicated that shaped holes performed as well as or better than cylindrical holes in every case.

Discharge coefficients were measured for unblocked and blocked holes. Shaped holes with the $t/D = 0.9$ blockage were found to have discharge coefficients nearly identical to unblocked cylindrical holes, even though this shaped hole blockage gave an effective AR that was 20% greater than cylindrical holes.

Area-averaged adiabatic effectiveness scaled with an effective momentum flux ratio, evaluated using the flow velocity at the exit of the coolant hole. Peak effectiveness was found to occur near an effective momentum flux ratio of 0.2 for shaped holes, regardless of blockage geometry. A relationship was found between the percent reduction in adiabatic effectiveness and the effective momentum flux ratio that was insensitive to blockage size, DR, and blowing ratio.

This relationship may simplify the work of the gas turbine designer by allowing the designer to estimate film cooling degradation for partial hole blockages. The effective momentum flux ratio (I_{eff}) for blocked holes can be calculated from the expected effective AR and flow conditions. To estimate the blocked hole effectiveness, the presented trendlines can be used to find film cooling performance with a blockage.

Acknowledgment

The authors are grateful to United Technologies—Pratt & Whitney and the NASA Aeronautics Scholarship Program for support of this project. We also would like to thank Jeff Glusman at Penn State, who helped develop our spraying process for the foam blockages.

Nomenclature

A = hole cross-sectional area (m^2)
AR = area ratio ($A_{\text{exit}}/A_{\text{inlet}}$)
APS = air-plasma spray
c = streamwise length of blockage top surface (m)
C_d = discharge coefficient ($\dot{m}/A_{\text{inlet}}[2\rho_c(p_{t,c} - p_\infty)]^{0.5}$)
D = diameter of film cooling holes (m)
DR = density ratio (ρ_c/ρ_∞)
I = momentum flux ratio ($\rho_c U_c{}^2/\rho_\infty U_\infty{}^2$)
k = thermal conductivity (W/m·K)
L = injection hole length (m)
M = blowing ratio ($\rho_c U_c/\rho_\infty U_\infty$)
$\dot{m}$ = coolant mass flow rate (kg/s)
p = pressure (Pa)
P = lateral distance between holes, pitch (m)
PR = pressure ratio ($p_{t,c}/p_\infty$)
Re = Reynolds number
t = coating thickness (m)
T = temperature (K)
TBC = thermal barrier coating
U = velocity (m/s)
w = breakout width (m)
x = streamwise distance measured from the unblocked hole downstream edge (m)

Greek Symbols

α = hole injection angle (deg)
β = expansion angle for shaped hole diffused outlet (deg)
δ = 99% boundary layer thickness (m)
η = local adiabatic effectiveness, $(T_\infty - T_{aw})/(T_\infty - T_c)$
θ = momentum thickness (m)
ρ = fluid density (kg/m^3)

Subscripts

aw = adiabatic wall
b, ub = blocked, unblocked
c = coolant, at hole inlet
CL = centerline
eff = effective, at hole exit
exit = exit plane of the film cooling hole
fwd = forward expansion of shaped hole
inlet = inlet plane of the film cooling hole
lat = lateral expansion of shaped hole (half-angle)
t = total
∞ = freestream
θ = based on the momentum thickness

Superscripts

$\bar{}$ = laterally averaged
$\bar{\bar{}}$ = area-averaged
* = based on the friction velocity

References

[1] Bunker, R. J., 2000, "Effect of Partial Coating Blockage on Film Cooling Effectiveness," ASME Paper No. 2000-GT-0244.
[2] Bogard, D. G., Schmidt, D. L., and Tabbita, M., 1998, "Characterization and Laboratory Simulation of Turbine Airfoil Surface Roughness and Associated Heat Transfer," ASME J. Turbomach., **120**(2), pp. 337–342.
[3] Jovanovic, M. B., de Lange, H. C., and van Steenhoven, A. A., 2005, "Influence of Laser Drilling Imperfection on Film Cooling Performances," ASME Paper No. GT2005-68251.
[4] Demling, P., and Bogard, D. G., 2006, "The Effects of Obstructions on Film Cooling Effectiveness on the Suction Side of a Gas Turbine Vane," ASME Paper No. GT2006-90577.
[5] Sundaram, N., and Thole, K. A., 2007, "Effects of Surface Deposition, Hole Blockage, and Thermal Barrier Coating Spallation on Vane Endwall Film Cooling," ASME J. Turbomach., **129**(3), pp. 599–607.
[6] Na, S., Cunha, F. J., Chyu, M. K., and Shih, T. I.-P., 2006, "Effects of Coating Blockage and Deposit on Film-Cooling Effectiveness and Surface Heat Transfer," AIAA Paper No. 2006-0024.
[7] Eberly, M. K., and Thole, K. A., 2014, "Time-Resolved Film-Cooling Flows at High and Low Density Ratios," ASME J. Turbomach., **136**(6), p. 061003.
[8] Schroeder, R. P., and Thole, K. A., 2013, "Shaped Hole Literature Review Database," Penn State Experimental and Computational Convection Laboratory (ExCCL), University Park, PA, avaiilable at: http://www.mne.psu.edu/psuturbine/
[9] Schroeder, R. P., and Thole, K. A., 2014, "Adiabatic Effectiveness Measurements for a Baseline Shaped Film Cooling Hole," ASME Paper No. GT2014-25992.
[10] Thole, K. A., Sinha, A. K., Bogard, D. G., and Crawford, M. E., 1992, "Mean Temperature Measurements of Jets With a Crossflow for Gas Turbine Film Cooling Application," *Rotating Machinery Transport Phenomena*, J. H. Kim, and W. J. Yang, eds., Hemisphere, New York.
[11] Sinha, A. K., Bogard, D. G., and Crawford, M. E., 1991, "Film Cooling Effectiveness Downstream of a Single Row of Holes With Variable Density Ratio," ASME J. Turbomach., **113**(3), pp. 442–449.
[12] Figliola, R. S., and Beasley, D. E., 2006, *Theory and Design for Mechanical Measurements*, Wiley, Hoboken, NJ.
[13] Burd, S. W., and Simon, T. W., 1999, "Measurements of Discharge Coefficients in Film Cooling," ASME J. Turbomach., **121**(2), pp. 243–248.
[14] Demling, P. D. R., 2005, "The Effects of Obstructions on Film Cooling Effectiveness on the Suction Side of a Gas Turbine Vane," Master's thesis, The University of Texas at Austin, Austin, TX.